Biochemical and Biophysical Research Communications **280,** 249–258 (2001)
doi:10.1006/bbrc.2000.4109, available online at http://www.idealibrary.com on IDEAL®

Deranged Expression of Molecular Chaperones in Brains of Patients with Alzheimer's Disease

Byong Chul Yoo,* Seong Hwan Kim,* Nigel Cairns,† Michael Fountoulakis,‡ and Gert Lubec*
**Department of Pediatrics, University of Vienna, Vienna, Austria; †Institute of Psychiatry, Brain Bank, King's College, London, United Kingdom; and ‡Pharmaceutical Research, Genomics Technologies, F. Hoffmann-La Roche, Ltd., Basel, Switzerland*

Received December 1, 2000

Alzheimer's disease (AD) is one of the disorders caused by protein conformational changes and recent studies have shown that several chaperone proteins are involved in this process. As information of chaperone expression in AD brain is limited, we aimed to study the expressional pattern of chaperones in several brain regions, as this may be essential to understand how folding defects can lead to disease. We studied the concomitant expressional patterns of molecular chaperones in seven brain regions of adults with AD using two-dimensional polyacrylamide gel electrophoresis (2-DE) and matrix-associated laser desorption ionization mass spectroscopy (MALDI-MS). We unambiguously identified and quantified nine different chaperone proteins. Six chaperone proteins, heat shock protein 60 (HSP 60), HSP 70 RY, heat shock cognate (HSC) 71, alpha crystallin B chain, glucose regulated protein (GRP) 75, and GRP 94 showed aberrant expressional patterns depending on brain region. HSP 70.1, GRP 78 and T-complex 1 (TCP-1) epsilon subunit did not show any significant expressional change. These findings are compatible with neuropathological and biochemical abnormalities in AD brain and this report presents the first approach to quantify nine different chaperones simultaneously at the protein level in individual AD brain regions providing evidence for the relevance of aberrant chaperone expression to AD neuropathology. © 2001 Academic Press

Key Words: **Alzheimer's disease; molecular chaperones; heat shock proteins; glucose regulated proteins; brain.**

Abbreviations used: Aβ, amyloid β peptide; AD, Alzheimer's disease; APP, amyloid precursor protein; GRP, glucose regulated protein; HSP, heat shock protein; MALDI-MS, matrix-associated laser desorption ionization mass spectroscopy; TCP-1, T-complex protein 1; 2-DE, two-dimensional gel electrophoresis.

It is generally accepted that several diverse disorders have the same molecular basis: a change in protein conformation. These protein conformational diseases include Alzheimer's disease (AD), prion-related disorders, systemic amyloidosis, serpin-deficiency disorders, Huntington's disease, and amyotrophic lateral sclerosis (1–3). The hallmark event in protein conformational disorders is a change in the secondary and tertiary structure of a normal protein without alteration in the primary structure and recently, many reports have shown that molecular chaperones appear to play a role in this conformational change (1–3).

In the case of AD, most molecular chaperone studies have focused on their role in amyloid fibril formation. The deposition of amyloid β peptide (Aβ) in extracellular plaques in the central nervous system and in the walls of cerebral blood vessels is the main histological characteristic of AD (4, 5). Aβ is derived by proteolytic processing of the amyloid precursor protein (APP), a transmembrane protein of unknown function. The biological activity of Aβ correlates with its conformational state. Monomeric Aβ_{1-40} or Aβ_{1-42} is in a random coil or α-helical conformation and stimulates neuronal outgrowth *in vitro* (6). A change into β-sheet conformation leads to the multistep assembly of fibrils (7) and a concomitant toxic effect towards neurons *in vitro* (8).

Small heat shock proteins (sHSPs) HSP 27 and alpha crystallin B are most well studied in AD and the expression of these chaperones has been proposed to reflect the defensive response to diminish amyloid fibril formation and subsequent toxicity (9, 10). Like sHSPs, HSP 40, and HSP 70 have been reported to inhibit self-assembly of poly-glutamine proteins into amyloid like fibrils (11). Furthermore, recent studies revealed that glucose regulated protein (GRP) 78 also binds to APP and decrease Aβ_{1-40} and Aβ_{1-42} secretion (12). In contrast to other chaperones, different functions of HSC 73 and HSP 90 appear to be involved in proteasome function and especially HSC 73 effectively interacts with cytoplasmic domain of APP in the pres-

0006-291X/01 $35.00
Copyright © 2001 by Academic Press
All rights of reproduction in any form reserved.

ence of proteasome inhibitors (13). These findings suggest that chaperones may function in the conformational maintenance of proteasome and also raises the possibility of aberrant protein recognition by proteasome.

Recently, the functions of several molecular chaperones in AD neuropathology have been suggested but unfortunately, very little is known about the expression patterns of individual molecular chaperones depending on AD brain regions. Since the expression of molecular chaperones under pathological conditions might be essential to understand how folding defects can lead to disease, we aimed to study the expression patterns of molecular chaperones, including several HSPs, GRPs, and chaperonins, in seven brain regions of adults with AD using two-dimensional polyacrylamide gel electrophoresis (2-DE) and matrix-associated laser desorption ionization mass spectroscopy (MALDI-MS).

In this paper we report aberrant expressional patterns of molecular chaperones compatible with histo-neuropathological and biochemical abnormalities present in the brain of AD patients and discuss the relevance of their expression to AD neuropathology.

MATERIALS AND METHODS

Human brain sample. Seven individual brain regions (frontal, temporal, parietal and occipital cortex, cerebellum, thalamus, and caudate nucleus) were obtained from the Medical Research Council's London Brain Bank for Neurodegenerative Diseases, Department of Neuropathology, Institute of Psychiatry (London, UK). The major cause of death in AD patients was bronchopneumonia. Age-matched controls were individuals with no history of neurological or psychiatric illness and the major cause of death was heart disease. AD patients satisfied the National Institute of Neurological and Communicative Disorders and Stroke and the Alzheimer Disease and Related Disorders Association (NINCDS/ADRDA) criteria for probable AD (14). The historical diagnosis of AD was established consistent with the CERAD criteria (15) for a 'definite' diagnosis of AD. Brain pH was measured essentially as reported (16). Since all not samples was available in seven individual brain regions and in a few 2-D gels, some protein spots were not clearly separated, detailed information of samples used in the determination of molecular chaperone expression level is summarized in Table 1. All samples were stored at −70°C until use.

Two-dimensional gel electrophoresis. Brain tissue was suspended in 0.5 ml of sample buffer consisting of 40 mM Tris, 5 M urea (Merck, Darmstadt, Germany), 2 M thiourea (Sigma, St. Louis, MO), 4% Chaps (Sigma), 10 mM 1,4-dithioerythritol (Merck), 1 mM EDTA (Merck) and a mixture of protease inhibitors, 1 mM PMSF and 1 μg of each pepstatin A, chymostatin, leupeptin, and antipain. The suspension was sonicated for approximately 30 s and centrifuged at 100,000*g* for 10 min and the supernatant was centrifuged further at 150,000*g* for 45 min. The protein content in the supernatant was determined by the Coomassie blue method (17). The 2-DE was performed essentially as reported (18). Samples of 1.5 mg were applied on immobilized pH 3–10 nonlinear gradient strip (IPG, Pharmacia Biotechnology, Uppsala, Sweden), at both, the basic and acidic ends of the strips. The proteins were focused at 3500 V within 6 h. Focusing was continued at 5000 V for 48 h. The second-dimensional separation was on 9–16% linear gradient polyacrylamide gels (chemicals from Serva, Heidelberg, Germany and Bio-Rad, Hercules, CA). The gels were stained with colloidal Coomassie blue (Novex, San Diego, CA) for 48 h, destained with water and scanned in a Molecular Dynamics Personal densitometer. The images were processed using Photoshop (Adobe) and PowerPoint (Microsoft) software. Protein spots were quantified using the ImageMaster 2D Elite software (Amersham Pharmacia Biotechnology).

Matrix-associated laser desorption ionization mass spectroscopy (MALDI-MS). MALDI-MS analysis was performed as described (19) with minor modifications. Briefly, spots were excised, destained with 50% acetonitrile in 0.1 M ammonium bicarbonate and dried in a speedvac evaporator. The dried gel pieces were reswollen with 3 μl of 3 mM Tris–HCl, pH 8.8, containing 50 ng trypsin (Promega, Madison, WI) and after 15 min, 3 μl of water were added. One microliter was applied onto the dried matrix spot. The matrix consisted of 15 mg nitrocellulose (Bio-Rad) and 20 mg α–cyano 4 hydroxycinnamic acid (Sigma) dissolved in 1 ml acetone:isopropanol (1:1, v/v). 0.5 μl of the matrix solution was applied on the sample target. Specimen were analyzed in a time-of-flight PerSeptive Biosystems mass spectrometer (Voyager Elite, Cambridge, MA) equipped with a reflectron. An accelerating voltage of 20 kV was used. Calibration was based upon the total optical density of all spots and the background. The peptide masses were matched with the theoretical peptide masses of all proteins from all species of the SWISS-PROT database. For protein search, monoisotopic masses were used and a mass tolerance of 0.0075% was allowed.

Statistical analyses. Percentage densities of total protein were obtained from quantifying protein spots on 2-DE map. Between-group differences were calculated by non-parametric Mann-Whitney U-test and within-group-correlations were done using the Spearman rank-coefficient. The significance was set at the $P < 0.05$ level.

RESULTS

Identification and Quantification of Molecular Chaperones on 2-DE Map of Human Brain

Human proteins obtained from seven individual brain regions with no pH difference were applied on 2-D gel. The protein spots were visualized following stain with colloidal Coomassie blue. Figure 1 shows an example of brain proteins from the parietal cortex of one control, separated on 2-D gel. The protein spots were analysed by MALDI-MS, following in-gel digestion. The peptide masses were matched with the theoretical peptide masses of all proteins of the SWISS-PROT database (Table 2). We used internal standards to correct the measured peptide mass, reducing, thus, the windows of mass tolerance and increasing the confidence of identification. Approximately 120 proteins were identified (20) and among these proteins, nine molecular chaperones were quantified using the ImageMaster 2D Elite software. The expression levels of molecular chaperones were determined as a percentage of total proteins present in the gel part considered. In Fig. 1, nine molecular chaperones are labelled with their SWISS-PROT accession numbers and names.

The Effect of Sex, Age, and Postmortem Interval on the Molecular Chaperone Expression Levels in Three Study Groups

Linear regression analysis revealed that in each individual brain regions of three study groups sex, age,

TABLE 1

Sex, Age, and Postmortem Interval of Human Brain Samples Used in the Determination of the Levels of Nine Different Chaperone Proteins in Individual Brain Regions

I

		Alpha crystallin B			HSP 60			HSP 70.1		
		Sex (F/M)	Age (years)	Postmortem interval (hours)	Sex (F/M)	Age (years)	Postmortem interval (hours)	Sex (F/M)	Age (years)	Postmortem interval (hours)
Cerebellum	Control	(5/8)	46.00 ± 18.02	41.15 ± 18.61	(3/3)	50.50 ± 13.58	41.33 ± 24.54	(2/3)	45.80 ± 21.18	33.80 ± 9.60
	AD	(4/7)	60.00 ± 6.25	32.91 ± 27.38	(4/4)	58.50 ± 6.46	37.50 ± 30.95	(3/3)	61.33 ± 6.02	25.33 ± 11.27
Temporal cortex	Control	(3/11)	49.64 ± 17.45	38.57 ± 20.08	(2/11)	46.31 ± 16.46	36.69 ± 20.48	(2/11)	50.23 ± 15.73	39.08 ± 20.66
	AD	(4/7)	59.55 ± 6.11	32.46 ± 27.83	(3/7)	59.10 ± 6.24	32.90 ± 29.30	(2/7)	59.00 ± 6.69	34.89 ± 30.50
Frontal cortex	Control	(3/6)	56.00 ± 10.91	41.33 ± 21.77	(3/6)	56.00 ± 10.91	41.33 ± 21.77	(3/4)	56.86 ± 12.10	41.57 ± 22.75
	AD	(3/4)	57.43 ± 6.37	36.14 ± 33.45	(3/3)	57.00 ± 6.87	38.00 ± 36.25	(0/3)	58.33 ± 7.64	14.67 ± 8.96
Occipital	Control	(5/9)	49.50 ± 16.46	39.93 ± 20.88	(3/6)	46.89 ± 15.19	42.78 ± 23.25	(4/4)	44.88 ± 19.20	35.00 ± 21.71
	AD	(3/7)	61.80 ± 7.16	26.10 ± 19.16	(4/6)	58.70 ± 5.72	33.00 ± 29.28	(3/6)	59.78 ± 4.87	26.00 ± 20.32
Parietal cortex	Control	(2/5)	56.00 ± 6.00	41.86 ± 25.05	(2/5)	56.00 ± 6.00	41.86 ± 25.05	(2/3)	57.20 ± 5.93	42.40 ± 27.73
	AD	(2/4)	59.50 ± 4.97	22.67 ± 13.88	(2/3)	61.00 ± 1.41	23.40 ± 14.01	(2/4)	59.83 ± 5.46	39.33 ± 29.04
Thalamus	Control	(2/8)	45.90 ± 20.00	35.10 ± 15.77	(2/7)	46.67 ± 19.08	34.89 ± 16.71	(1/7)	46.88 ± 19.25	33.25 ± 17.15
	AD	(1/6)	60.28 ± 6.40	21.43 ± 22.66	(0/7)	57.43 ± 9.31	22.57 ± 22.72	(0/7)	57.43 ± 9.31	22.57 ± 22.72
Caudate nucleus	Control	(1/4)	53.20 ± 13.61	23.40 ± 8.41	(1/5)	45.00 ± 20.95	34.33 ± 11.66	(1/5)	45.00 ± 20.95	34.33 ± 11.66
	AD	(2/6)	61.13 ± 6.03	27.13 ± 21.06	(2/4)	61.83 ± 4.02	30.00 ± 23.50	(2/5)	60.14 ± 5.79	27.14 ± 22.75

II

		HSP 70 RY			HSC 71			TCP-1 epsilon subunit		
		Sex (F/M)	Age (years)	Postmortem interval (hours)	Sex (F/M)	Age (years)	Postmortem interval (hours)	Sex (F/M)	Age (years)	Postmortem interval (hours)
Cerebellum	Control	(4/6)	43.30 ± 19.07	38.30 ± 14.61	(2/2)	60.00 ± 13.09	42.00 ± 13.37	(4/5)	48.00 ± 18.98	44.78 ± 19.87
	AD	(4/6)	59.80 ± 6.55	31.80 ± 28.60	(2/1)	62.67 ± 1.16	32.00 ± 10.58	(4/3)	55.83 ± 9.37	37.50 ± 30.95
Temporal cortex	Control	(3/12)	49.07 ± 16.96	38.13 ± 19.42	(1/10)	48.55 ± 15.82	38.09 ± 21.52	(0/9)	54.00 ± 9.70	34.78 ± 19.05
	AD	(4/5)	59.22 ± 6.76	32.00 ± 30.73	(3/7)	59.10 ± 6.24	32.90 ± 29.30	(3/6)	60.67 ± 5.59	26.22 ± 20.32
Frontal cortex	Control	(2/5)	57.57 ± 11.98	32.86 ± 14.38	(2/4)	55.67 ± 12.81	38.83 ± 23.62	(3/6)	56.00 ± 10.91	41.33 ± 21.77
	AD	(3/4)	57.43 ± 6.37	36.14 ± 33.45	(2/4)	58.83 ± 5.67	26.16 ± 22.52	(2/2)	53.75 ± 5.91	48.75 ± 41.11
Occipital cortex	Control	(5/6)	48.64 ± 17.80	40.46 ± 20.60	(4/4)	49.50 ± 16.97	41.25 ± 25.11	(4/7)	46.82 ± 17.46	41.82 ± 21.18
	AD	(4/7)	59.55 ± 6.11	32.46 ± 27.83	(4/5)	58.67 ± 6.06	36.11 ± 29.25	(3/7)	59.30 ± 6.38	33.30 ± 29.19
Parietal cortex	Control	(2/4)	57.33 ± 5.32	39.00 ± 26.16	(2/3)	57.20 ± 5.93	42.40 ± 27.73	(2/5)	56.00 ± 6.00	41.86 ± 25.05
	AD	(4/3)	58.43 ± 6.21	35.14 ± 28.73	(3/4)	59.85 ± 4.63	22.14 ± 12.75	(1/3)	60.75 ± 1.50	24.50 ± 15.93
Thalamus	Control	(2/7)	43.67 ± 19.85	31.56 ± 11.76	(2/7)	43.89 ± 20.12	33.78 ± 16.12	(1/7)	52.25 ± 16.85	34.50 ± 17.82
	AD	(1/7)	52.17 ± 4.62	22.13 ± 21.07	(0/7)	57.43 ± 9.31	22.57 ± 22.72	(1/7)	58.00 ± 8.77	22.13 ± 21.07
Caudate nucleus	Control	(2/7)	43.67 ± 19.85	31.56 ± 11.76	(1/5)	45.00 ± 20.95	34.33 ± 11.66	(1/5)	41.33 ± 18.77	31.00 ± 10.06
	AD	(2/6)	61.13 ± 6.03	27.13 ± 21.06	(2/6)	59.50 ± 6.06	27.13 ± 21.06	(2/3)	61.80 ± 4.49	27.20 ± 25.13

III

		GRP 75			GRP 78			GRP 94		
		Sex (F/M)	Age (years)	Postmortem interval (hours)	Sex (F/M)	Age (years)	Postmortem interval (hours)	Sex (F/M)	Age (years)	Postmortem interval (hours)
Cerebellum	Control	(2/1)	58.67 ± 15.70	36.67 ± 9.87	(4/5)	42.56 ± 20.12	41.00 ± 12.58	(2/3)	54.20 ± 17.09	32.20 ± 15.07
	AD	(3/1)	63.25 ± 1.50	20.00 ± 8.21	(3/5)	60.88 ± 5.94	28.88 ± 19.99	(3/4)	61.43 ± 5.62	20.43 ± 7.68
Temporal cortex	Control	(2/8)	48.80 ± 17.31	36.70 ± 19.17	(2/11)	50.23 ± 15.73	39.08 ± 20.66	(2/12)	48.79 ± 17.56	34.93 ± 15.50
	AD	(1/4)	57.20 ± 8.76	32.17 ± 24.41	(3/6)	58.67 ± 6.42	36.00 ± 29.61	(4/5)	52.85 ± 18.93	32.00 ± 30.73
Frontal cortex	Control	(2/3)	53.40 ± 12.87	41.80 ± 25.13	(3/5)	55.75 ± 11.63	43.75 ± 21.95	(3/6)	56.00 ± 10.91	41.33 ± 21.77
	AD	(1/4)	58.20 ± 6.10	25.40 ± 16.59	(2/4)	56.67 ± 6.62	39.00 ± 35.70	(2/4)	56.67 ± 6.62	38.17 ± 36.17
Occipital cortex	Control	(3/2)	40.60 ± 15.45	35.80 ± 27.79	(5/6)	48.82 ± 17.98	42.18 ± 22.05	(4/6)	48.20 ± 18.70	36.20 ± 15.82
	AD	(1/2)	58.67 ± 4.16	38.00 ± 27.88	(3/6)	61.11 ± 7.24	26.00 ± 20.32	(2/7)	60.44 ± 5.57	26.33 ± 20.31
Parietal cortex	Control	(2/2)	58.75 ± 5.56	49.25 ± 26.69	(2/4)	55.67 ± 6.50	45.17 ± 25.71	(2/4)	57.33 ± 5.32	39.00 ± 26.16
	AD	(3/3)	61.50 ± 1.76	24.14 ± 12.67	(4/4)	58.50 ± 5.76	31.38 ± 28.66	(4/4)	58.50 ± 5.76	31.38 ± 28.66
Thalamus	Control	(1/7)	46.88 ± 19.25	33.25 ± 17.15	(2/8)	45.90 ± 20.00	35.10 ± 15.77	(2/7)	43.67 ± 19.85	36.56 ± 11.76
	AD	(0/7)	57.43 ± 9.31	22.57 ± 22.72	(0/7)	57.43 ± 9.31	22.57 ± 22.72	(1/7)	58.00 ± 8.77	22.13 ± 21.07
Caudate nucleus	Control	(1/5)	45.00 ± 20.95	34.33 ± 11.66	(2/5)	41.43 ± 21.33	35.00 ± 10.89	(2/7)	43.67 ± 19.85	31.56 ± 11.76
	AD	(2/4)	61.17 ± 5.60	34.33 ± 11.66	(2/6)	61.13 ± 6.03	27.13 ± 21.06	(2/6)	61.13 ± 6.03	27.13 ± 21.06

Note. Values in the columns of 'Age' and 'Postmortem interval' indicate the means and standard deviations of samples used in present study. The table shows any statistical differences of age and postmortem interval in AD individual brain regions as compared to the control group.

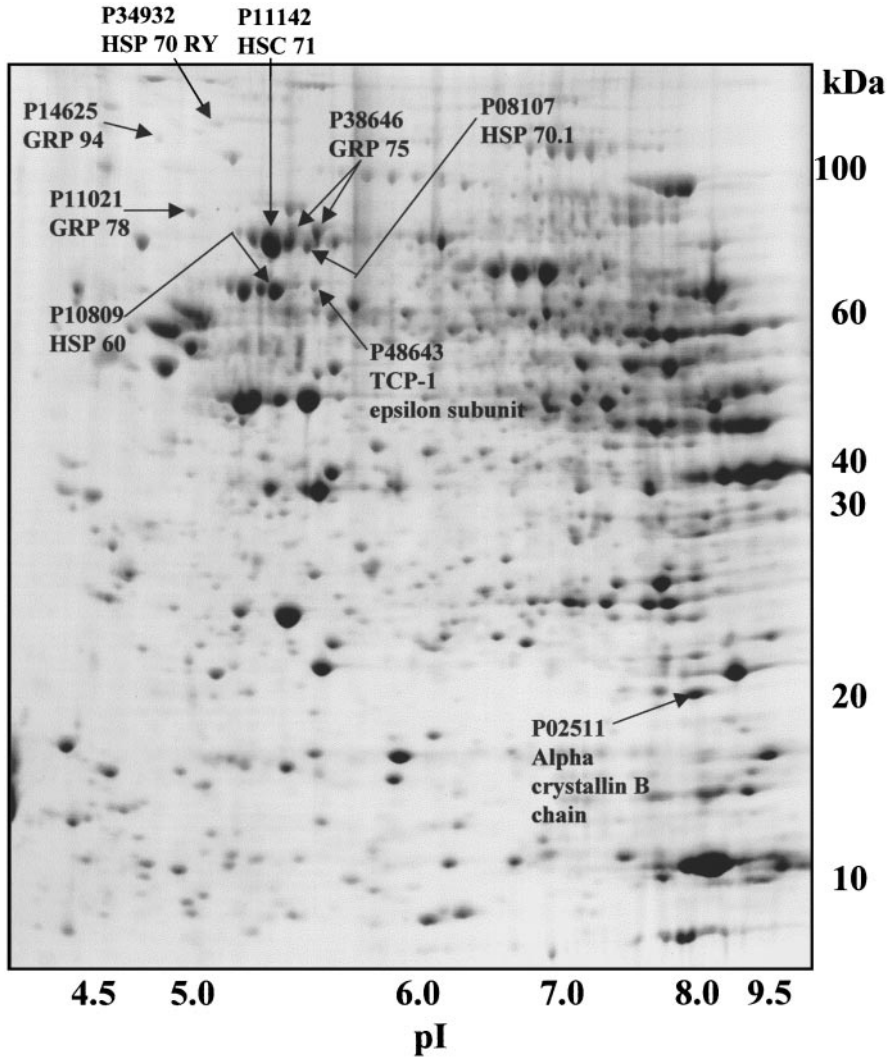

FIG. 1. 2-DE map of human brain proteins obtained from parietal cortex of a control. The 2-DE was performed in an immobilized pH 3-10 nonlinear gradient strip, followed by the second-dimensional separation on 9–16% linear gradient polyacrylamide gels, and separated proteins were detected by colloidal Coomassie blue staining. Approximately 120 spots were analyzed by MALDI-MS. Identified molecular chaperones are designated with their SWISS-PROT accession numbers and the names referring to Table 2.

and postmortem interval had no effect on the expression levels of all nine molecular chaperones studied (data not shown).

The Variable Expression Patterns of Molecular Chaperones in Seven Individual Brain Regions of Control Group

All molecular chaperones studied showed even expression patterns in control individual brain regions (Fig. 2). A comparison between the intensities of the spots representing each molecular chaperone showed that HSP 70 RY and GRP 94 were moderately expressed, whereas HSC 71 was highly expressed in all individual brain regions of control group (Figs. 1 and 2). In contrast to all other chaperone proteins studied, GRP 75 was represented by two spots with different pI (Figs. 1 and 4). Levels of GRP 75 in Figs. 2 and 3 represent sum of intensities of these two spots.

Abnormality of the Molecular Chaperone Expression in AD Brain

HSP 70.1, GRP 78 and T-complex 1 (TCP-1) epsilon subunit showed a comparable expression pattern in all individual AD brain regions to those of control group (Figs. 3C, 3G, and 3I). In AD temporal cortex HSC 71 and GRP 75 were significantly reduced (both $P < 0.05$) (Figs. 3E, 3F, and 4), whereas alpha crystallin B was increased ($P < 0.01$) (Figs. 3A and 4). In AD parietal cortex HSP 60 and GRP 75 were significantly decreased ($P < 0.05$ and $P < 0.01$, respectively) (Figs. 3B and 3F), whereas GRP 94 showed increased expression patterns ($P < 0.05$) (Fig. 3H). HSP 70 RY showed

TABLE 2

Mass Spectrometry Analysis of Nine Different Molecular Chaperone Proteins

							MALDI-MS		
			Mr		pI		Peptide		Sequence
No.[a]	Abbr. name	Protein name	Theor.	Observ.	Theor.	Observ.	Matching	Total	Coverage
P02511	CRAB_HUMAN	Alpha crystalline B chain	20,146	21,000	7.4	8.3	7	20	44
P08107	HS71_HUMAN	Heat shock 70 kDa protein 1 (HSP 70.1)	70,294	65,000	5.4	5.6	9	19	17
P10809	P60_HUMAN	Mitochondrial matrix protein P1 (HSP 60)	61,187	58,000	5.6	5.5	10	20	26
P11021	GR78_HUMAN	78 kDa glucose regulated protein (GRP 78)	72,185	77,000	4.9	5.0	10	19	18
P11142	HS7C_HUMAN	Heat shock cognate 71 kDa protein (HSC 71)	71,082	70,000	5.3	5.4	6	19	14
P14625	ENPL_HUMAN	Endoplasmin (94 kDa glucose regulated protein) (GRP 94)	92,696	100,000	4.6	4.8	9	20	20
P34932	HS74_HUMAN	Heat shock 70 kDa protein 4 (HSP 70 RY)	79,857	105,000	5.0	5.2	8	20	13
P38646	GR75_HUMAN	75 kDa glucose regulated protein (GRP 75)	74,018	69,000	6.2	6.5	8	20	15
P48643	TCPE_HUMAN	T-complex protein 1, epsilon subunit (TCP-1-epsilon) (KIAA0098)	60,088	58,000	5.4	5.6	7	18	15

Note. The protein spots were excised from the gels, digested with trypsin and the peptides generated were analyzed by MALDI-MS as stated under Materials and Methods. The identified protein spots are characterized by their SWISS-PROT accession numbers as indicated in Fig. 1. The theoretical and the approximate observed Mr and pI values, as well as the matching and total peptides and the protein sequence coverage by the matching peptides are given.

[a] SWISS-PROT accession number.

an increase in AD caudate nucleus ($P < 0.01$) (Fig. 3D).

DISCUSSION

Amyloid plaques contain besides Aβ several other proteins, including the sHSPs alpha crystallin B and HSP 27 (9, 10). Both are molecular chaperones that are able to prevent aggregation of other proteins and the expression of these sHSPs in AD has been proposed to represent a defensive response to diminish amyloid fibril formation and subsequent toxicity (21, 22). Alpha crystallin B does prevent the fibrillization of Aβ_{1-40}, however, it induces alpha crystallin B/Aβ complexes that are highly neurotoxic. This suggested that alpha crystallin B was involved in the pathogenesis of AD by influencing the process of amyloid toxicity. Shinohara and co-workers reported that the concentration of alpha crystallin B was elevated in temporal and frontal cortex of AD brains, using specific immunoassays for alpha crystallin B (9). Increased expression of alpha crystallin B has been reported in reactive astrocytes, microglia, and oligodendrocytes (9, 10). Because of co-localization of glial fibrillary acidic protein (GFAP) and alpha crystallin B in fibrous astrocytes (10), our finding of increased alpha crystallin B in AD temporal cortex may reflect reactive gliosis as well as reactive mechanism to reduce fibrill of Aβ_{1-40}.

The APP gene promoter contains a heat shock element and abnormal APP heat shock response can increase accumulation of Aβ, the APP metabolite found in AD amyloid plaques (23, 24). HSP 70-induced APP mRNA suggested a role of heat shock response for the induction of APP (25). Furthermore, the role of HSPs in Aβ formation has been suggested following the observation that HSP 70 and HSP 40 chaperones inhibit self-assembly of polyglutamine proteins into amyloid-like fibrils (11) and HSC 73 (also known as HSC 71) effectively interacts with the cytoplasmic domain of APP in the presence of proteasome inhibitors (13). Kouchi and co-workers showed that HSC 73 is involved in a proteasome complex and reduction of protein degradation in mutant strains of HSP 70 genes and DnaJ homologue in yeast, suggesting functional role of HSC 73 in the conformational maintenance of proteasome (13). This finding also raises the possibility that HSPs may contribute to the conformational recognition of aberrant proteins by proteasome. These observations indicate the crucial role of HSPs in impeding AD progression and their downregulation as shown by our results appears to create a gap in the whole system. In contrast to all other chaperone proteins studied, GRP

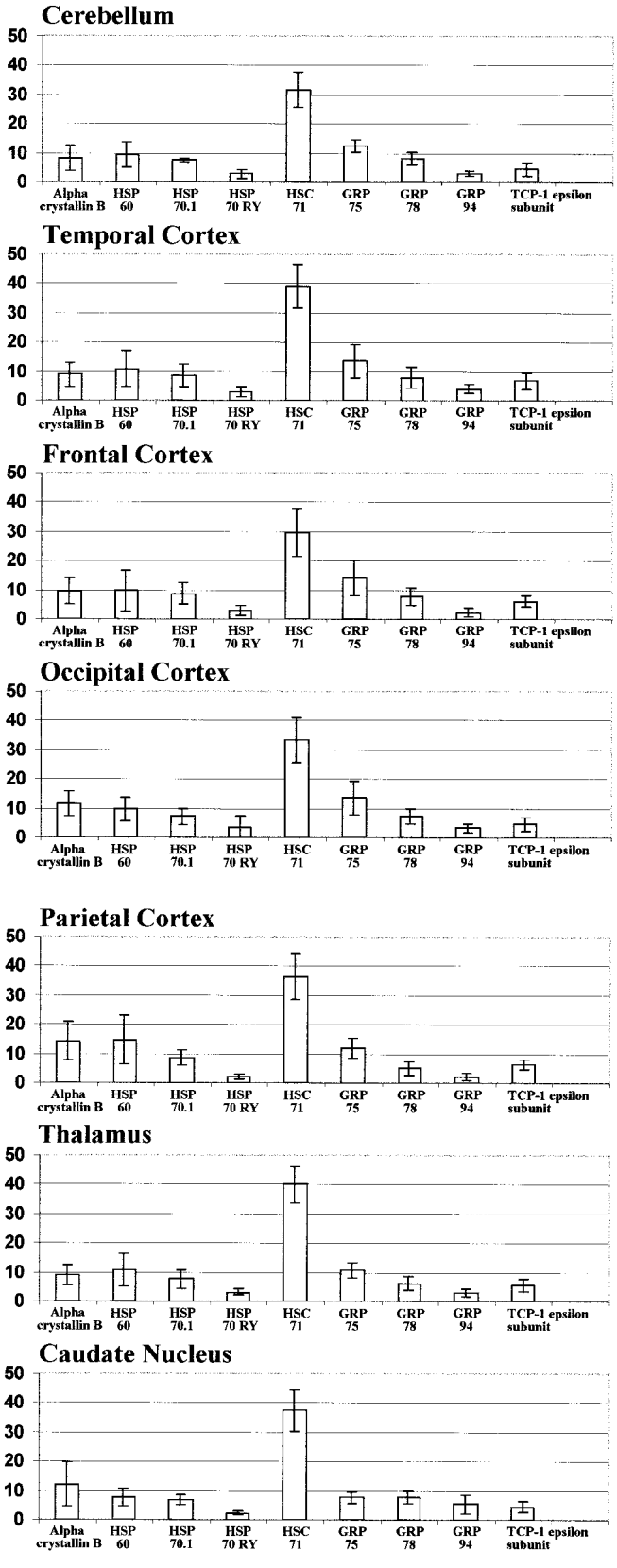

FIG. 2. The expression patterns of nine molecular chaperones in individual brain regions of control. The expressions of nine molecular chaperones on 2-DE gels obtained from seven individual control brain regions i.e., frontal, temporal, parietal, occipital cortex, cerebellum, thalamus, and caudate nucleus were quantified using the ImageMaster 2D Elite software. Molecular chaperone expressional level was determined as the percentage volume of total proteins present in the gel part considered. All nine molecular chaperones were evenly expressed in seven individual brain regions. The columns and bars indicate means and standard deviations of the expression levels of each molecular chaperone.

75 was separated as two spots with different pI on 2-DE gel (Figs. 1 and 4). The two spots seem to be isoforms, probably obtained as a result of different phosphorylation and although their functional and physiological significance is unknown, it is interesting to note that each spot was evenly decreased in AD parietal and temporal cortex. With a notion that down-regulation or disruption of HSP 70 expression results in apoptosis, Mosser and co-workers (26) studied the role of HSP 70 in blocking the apoptotic process and showed its inhibitory effect on activation of the caspase protease cascade and signalling through the stress-activated protein kinase (SAPK)/c-Jun N-terminal kinase (JNK) pathway. Thus, taken together it is conceivable to assume that loss of HSP 70 family proteins particularly, HSC 71 and GRP 75, plays a greater role in neuronal death associated with AD.

Unlike HSC 71, HSP 70.1 didn't show any change in expression level in AD brain indicating that though each member of HSP 70 family presents with high homology and shares many functional roles in protein folding (27), the expression of HSP 70 individual members differentially respond to particular injury and in brain region (28). Furthermore, HSC 71 and HSP 70.1 show different gene localization suggesting different way of gene regulation (29, 30). As HSC 71 is mainly expressed in human brain amongst the HSP 70 family proteins, our findings strongly imply that HSC 71 and GRP 75 are the major HSP 70 members involved in AD pathology and temporal and parietal cortices are the most affected brain region by the abnormal expression of HSP 70 proteins as well as alpha crystallin B.

The increase in HSP 70 RY in AD caudate nucleus ($P < 0.01$) (Fig. 3D) points to an involvement of HSPs in a functional area, the basal ganglia. HSP 70 RY was identified as a member of the HSP 70 protein family on the basis of cDNA sequence homology (31) but its amino acid sequence diverges significantly from the other human HSP 70 proteins (32). Whether this divergence has impact on level of expression and the functional significance of our finding remains to be determined.

Even though GRP 75 and HSP 60 are both localized in mitochondria and facilitate the folding and assembly of proteins as they enter into mitochondria (33), GRP 75 was shown to be a member of the HSP 70 family of stress proteins while HSP 60 represents the mammalian equivalent of the bacterial GroEL protein based on

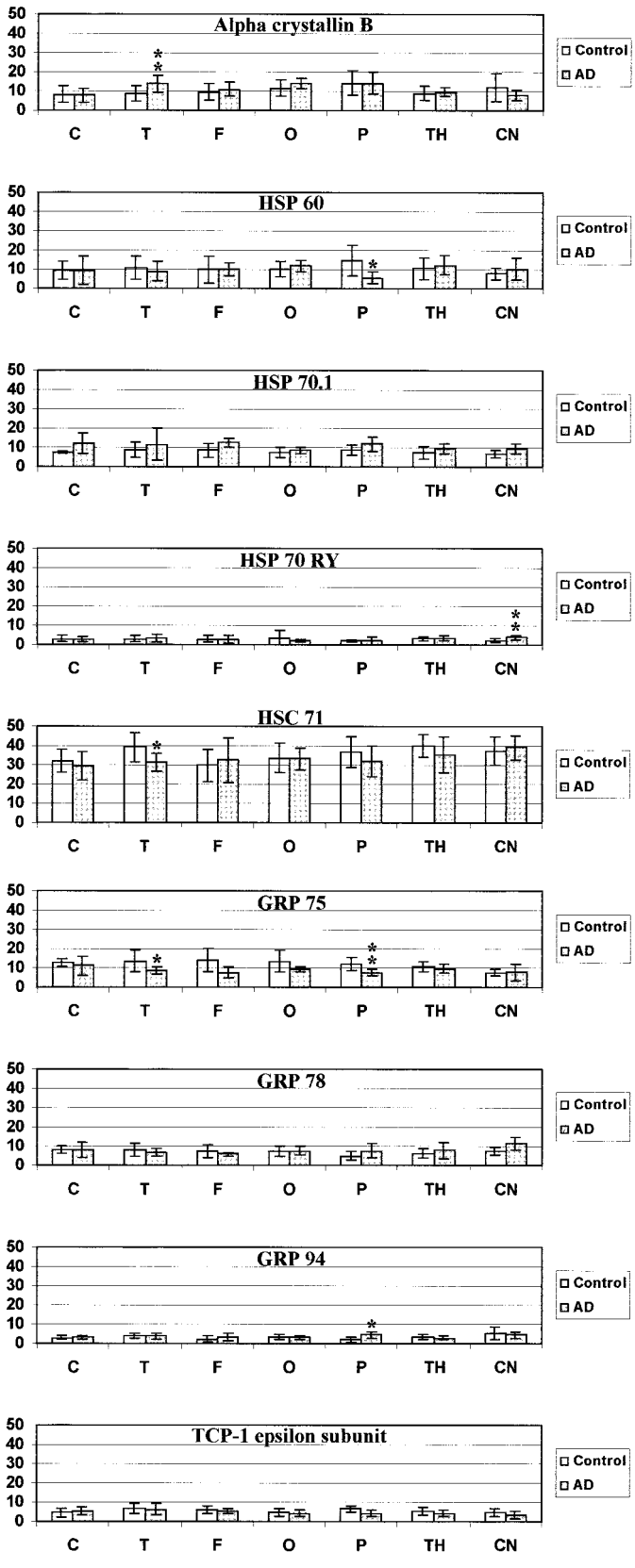

FIG. 3. Aberrant expressions of molecular chaperones in individual AD brain region. Nine molecular chaperones on the 2-DE gels from the corresponding brain regions of patients with AD and age-matched controls were quantified using the ImageMaster 2D Elite software and compared to each other employing non-parametric Mann-Whitney U-test in order to detect different expressional levels of those proteins. Molecular chaperone expressional level was determined as the percentage volume of total proteins present in the gel part considered. The columns and bars indicate the means and standard deviations of the expression levels of each molecular chaperone. Quantitative analysis was performed in seven individual brain regions: frontal(F), temporal (T), parietal (P), occipital cortex (O), cerebellum (C), thalamus (TH) and caudate nucleus (CN). In comparison with controls, $*P < 0.05$ and $**P < 0.01$ represent significantly increased or decreased expression.

a variety of biochemical and immunological criteria. Briones and co-workers suggested HSP 60 deficiency might be a common cause of mitochondrial disease (34). Oxidative stress and/or mitochondrial defect may represent the pathological hallmark of AD (35), furthermore expression of the human groEL stress-protein homologue such as HSP 60 in brain and spinal cord is consistent with a mitochondrial location and it provides a morphological indicator of the functional or metabolic state of cells (36). Our finding of low levels of both mitochondrial located chaperone proteins is in line with the mitochondrial defect proposed in AD brain.

The mature, healthy, nonstarved mammalian brain uses only glucose as a source of energy in the form of ATP (37). A reduction in the cerebral metabolic rate of glucose is one of the most predominant abnormalities generally found in the AD type brain (38). The cerebral dimunition in energy availability, along with a loss of functionally important amino acids, ammonia toxicity, supposed membrane damage, dysregulation of Ca^{2+} homeostasis, and glycogen accumulation in the incipient stages of dementia of the Alzheimer type (DAT) are assumed to be stress-related abnormalities capable of inducing the formation of heat shock proteins (39). These events may lead to an enhanced generation of APP in earlier states of DAT which in turn causes increased production of Aβ, if abnormally cleaved. Perturbation in brain oxidative energy and related metabolism may precede the generation of APP and the formation of plaques in the brain affected by incipient DAT. In this view, GRP 78 has been studied in AD brain; Hamos and co-workers reported that an increased expression of GRP 78 only in neurones of AD (40) and concerning a seminal role for $A\beta_{1-42}$ generation and aggregation in the ER in AD pathogenesis, Yang and co-workers suggested that GRP 78 binding to APP in neurons may have even greater functional consequences than in non-neuronal cells (12). Our finding shows no difference of GRP 78 expression in AD brain. In contrast to GRP 78, we found an increase of GRP 94 in AD parietal cortex. GRP 94 is a member of the HSP 90 family and HSP 90 was reported to form specific complexes with steroid hormone receptors and several protein kinases, including Raf (41) and Src (42). A

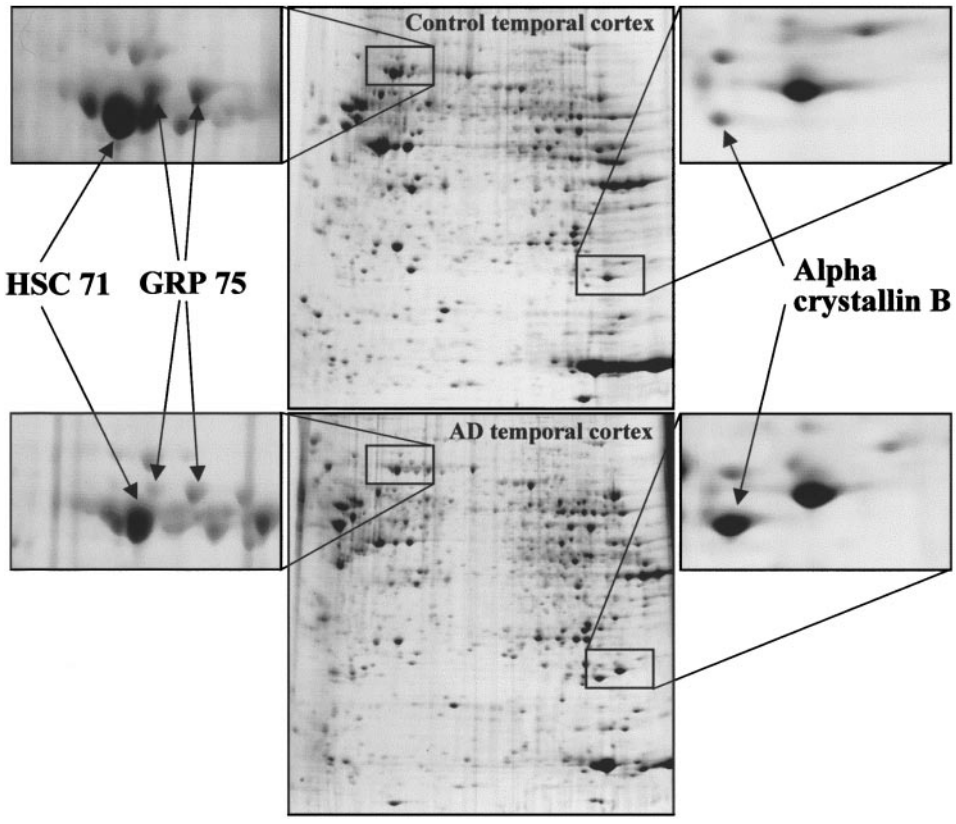

FIG. 4. Typical electrophoretic patterns of temporal protein extracts from control and AD. The 2-DE was performed in an immobilized pH 3–10 nonlinear gradient strip, followed by the second-dimensional separation on 9–16% linear gradient polyacrylamide gels, and separated proteins were detected by colloidal Coomassie blue staining. The entire gels show typical electrophoretic patterns and enlarged partial 2-DE images containing HSC 71, GRP 75 and alpha crystallin B spots demonstrate our findings (Figs. 3A, 3E, and 3F) of increased alpha crystallin B protein and decreased HSC 71 and GRP 75 proteins in temporal cortex of AD.

critical role has been suggested for HSP 90 in the regulation of the activity and intracellular translocation of these proteins (43). Importantly, HSP 90 has recently been suggested to mediate intracellular signal transduction events (44, 45). Nothing is known about the relevance of aberrant GRP 94 expression to AD pathology, likewise the functional significance of increased GRP 94 in AD brain pathology is still unanswered. However, based on above findings it seems plausible that increased GRP 94 may account for the abnormalities of intracellular translocation of protein kinases and intracellular signal transduction in AD brain (43–45).

We could not find any significant difference in expression levels of TCP-1 epsilon subunit. However, TCP-1 epsilon subunit showed decrease levels in AD parietal cortex although not reaching statistical significance (Fig. 3I). In interphase and mitotic cells TCP-1 is localized within the centrosome which serves as an initiation site for microtubule growth (46). Since TCP-1 is involved in microtubule growth, its mutation or abnormal expression may lead to mitotic and meiotic abnormalities of the cell cycle. If cell cycle regulatory mechanisms fail, the cell cycle is allowed to progress into the G_2 phase. Nagy suggested that the cell cycle in AD neurones can be arrested at the G_2/M transition point and at this point may undergo apoptosis via the p53/Bax related pathway (47). Interestingly, by a sensitive differential hybridization approach, Dittmar and co-workers showed the expression of TCP-1 appeared to be specifically linked with the S to G_2/M phase transition of the cell cycle (48). Furthermore, it was recently reported that the existence of a common mechanism of tumor suppression and apoptosis shared by p53, p21 (Waf1) and SIAH-1 involved regulation of TCP-1 (49). Thus, we may suggest that decreased TCP-1 expression in the AD parietal cortex may lead to arrest of brain cells at the G_2/M transition point and these cells may undergo apoptosis responsible for neuronal death in the AD parietal cortex.

In conclusion, the present results show the expressional patterns of nine different molecular chaperones in seven individual brain regions of AD patients. Five chaperone proteins, i.e., alpha crystallin B, HSP 60, HSC 71, GRP 75 and GRP 94 showed abnormal expression in parietal and temporal cortex, reflects regularly affected in AD brain pathology. These findings are compatible with neuropathological abnormalities

present in AD brain and our report represents the relevance of abnormal chaperone expression in AD brain pathology.

ACKNOWLEDGMENT

The authors at the University of Vienna are highly indebted to the Red Bull Company, Salzburg, for financial support of the study.

REFERENCES

1. Soto, C. (1999) Alzheimer's and prion disease as disorders of protein conformation: Implications for the design of novel therapeutic approaches. *J. Mol. Med.* **77**(5), 412–418.
2. Sifers, R. N. (1995) Defective protein folding as a cause of disease. *Nat. Struct. Biol.* **2**(5), 355–357.
3. Carrell, R. W., and Lomas, D. A. (1997) Conformational disease. *Lancet* **50**(9071), 134–138.
4. Selkoe, D. J. (1997) Alzheimer's disease: Genotypes, phenotypes, and treatments. S*cience* **275**(5300), 630–631.
5. Hardy, J., Duff, K., Hardy, K. G., Perez-Tur, J., and Hutton, M. (1998) Genetic dissection of Alzheimer's disease and related dementias: Amyloid and its relationship to tau. *Nat. Neurosci.* **1**(5), 355–358.
6. Pike, C. J., Burdick, D., Walencewicz, A. J., Glabe, C. G., and Cotman, C. W. (1993) Neurodegeneration induced by beta-amyloid peptides in vitro: the role of peptide assembly state. *J. Neurosci.* **13**(4), 1676–1687.
7. Kelly, J. W. (1998) The alternative conformations of amyloidogenic proteins and their multi-step assembly pathways. *Curr. Opin. Struct. Biol.* **8**(1), 101–106.
8. Lorenzo, A., and Yankner, B. A. (1994) Beta-amyloid neurotoxicity requires fibril formation and is inhibited by congo red. *Proc. Natl. Acad. Sci. USA* **91**(25), 12243–12247.
9. Shinohara, H., Inaguma, Y., Goto, S., Inagaki, T., and Kato, K. (1993) Alpha B crystallin and HSP28 are enhanced in the cerebral cortex of patients with Alzheimer's disease. *J. Neurol. Sci.* **119**(2), 203–208.
10. Renkawek, K., Voorter, C. E., Bosman, G. J., van Workum, F. P., and de Jong, W. W. (1994) Expression of alpha B-crystallin in Alzheimer's disease. *Acta Neuropathol. (Berl)* **87**(2), 155–160.
11. Muchowski, P. J., Schaffar, G., Sittler, A., Wanker, E. E., Hayer-Hartl, M. K., and Hartl, F. U. (2000) Hsp70 and hsp40 chaperones can inhibit self-assembly of polyglutamine proteins into amyloid-like fibrils. *Proc. Natl. Acad. Sci. USA* **97**(14), 7841–7846.
12. Yang, Y., Turner, R. S., and Gaut, J. R. (1998) The chaperone BiP/GRP78 binds to amyloid precursor protein and decreases Abeta40 and Abeta42 secretion. *J. Biol. Chem.* **273**(40), 25552–25555.
13. Kouchi, Z., Sorimachi, H., Suzuki, K., and Ishiura, S. (1999) Proteasome inhibitors induce the association of Alzheimer's amyloid precursor protein with Hsc73. *Biochem. Biophys. Res. Commun.* **254**(3), 804–810.
14. Tierney, M. C., Fisher, R. H., Lewis, A. J., Zorzitto, M. L., Snow, W. G., Reid, D. W., and Nieuwstraten, P. (1988) The NINCDS-ADRDA Work Group criteria for the clinical diagnosis of probable Alzheimer's disease: A clinicopathologic study of 57 cases. *Neurology* **38**(3), 359–364.
15. Mirra, S. S., Heyman, A., McKeel, D., Sumi, S. M., Crain, B. J., Brownlee, L. M., Vogel, F. S., Hughes, J. P., van Belle, G., and Berg, L. (1991) The Consortium to Establish a Registry for Alzheimer's Disease (CERAD). Part II. Standardization of the neuropathologic assessment of Alzheimer's disease. *Neurology* **41**(4), 479–486.
16. Lubec, B., Marx, M., Herrera-Marschitz, M., Labudova, O., Hoeger, H., Gille, L., Nohl, H., Mosgoeller, W., and Lubec, G. (1997) Decrease of heart protein kinase C and cyclin-dependent kinase precedes death in perinatal asphyxia of the rat. *FASEB. J.* **11**(6), 482–492.
17. Bradford, M. M. (1976) A rapid and sensitive method for the quantitation of microgram quantities of protein utilizing the principle of protein-dye binding. *Anal. Biochem.* **72,** 248–254.
18. Langen, H., Roder, D., Juranville, J. F., and Fountoulakis, M. (1997) Effect of protein application mode and acrylamide concentration on the resolution of protein spots separated by two-dimensional gel electrophoresis. *Electrophoresis* **18**(11), 2085–2090.
19. Fountoulakis, M., and Langen, H. (1997) Identification of proteins by matrix-assisted laser desorption ionization-mass spectrometry following in-gel digestion in low-salt, nonvolatile buffer and simplified peptide recovery. *Anal. Biochem.* **250**(2), 153–156.
20. Langel, H., Berndt, P., Roder, D., Cairns, N., Lubec, G., and Fountoulakis, M. (1999) Two-dimensional map of human brain proteins. *Electrophoresis* **20**(4–5), 907–916.
21. Horwitz, J. (1992) Alpha-crystallin can function as a molecular chaperone. *Proc. Natl. Acad. Sci. USA* **89**(21), 10449–10453.
22. Stege, G. J., Renkawek, K., Overkamp, P. S., Verschuure, P., van Rijk A. F., Reijnen-Aalbers, A., Boelens, W. C., Bosman, G. J., and de Jong, W. W. (1999) The molecular chaperone alphaB-crystallin enhances amyloid beta neurotoxicity. *Biochem. Biophys. Res. Commun.* **262**(1), 152–156.
23. Zhong, S., Wu, K., Black, I. B., and Schaar, D. G. (1996) Characterization of the genomic structure of the mouse APLP1 gene. *Genomics* **32**(1), 159–162.
24. Johnson, G., Refolo, L. M., and Wallace, W. (1993) Heat-shocked neuronal PC12 cells reveal Alzheimer's disease—associated alterations in amyloid precursor protein and tau. *Ann. NY Acad. Sci.* **695,** 194–197.
25. Abe, K., St George-Hyslop, P. H., Tanzi, R. E., and Kogure, K. (1991) Induction of amyloid precursor protein mRNA after heat shock in cultured human lymphoblastoid cells. *Neurosci. Lett.* **125**(2), 169–171.
26. Mosser, D. D., Caron, A. W., Bourget, L., Denis-Larose, C., and Massie, B. (1997) Role of the human heat shock protein hsp70 in protection against stress-induced apoptosis. *Mol. Cell. Biol.* **17**(9), 5317–5327.
27. Rajdev, S., and Sharp, F. R. (2000) Stress proteins as molecular markers of neurotoxicity. *Toxicol. Pathol.* **28**(1), 105–112.
28. Tavaria, M., Gabriele, T., Anderson, R. L., Mirault, M. E., Baker, E., Sutherland, G., and Kola, I. (1995) Localization of the gene encoding the human heat shock cognate protein, HSP73, to chromosome 11. *Genomics* **29**(1), 266–268.
29. Milner, C. M., and Campbell, R. D. (1990) Structure and expression of the three MHC-linked HSP70 genes. *Immunogenetics* **32**(4), 242–251.
30. Dworniczak, B., and Mirault, M. E. (1987) Structure and expression of a human gene coding for a 71 kd heat shock 'cognate' protein. *Nucleic Acids Res.* **15**(13), 5181–5197.
31. Fathallah, D. M., Cherif, D., Dellagi, K., and Arnaout, M. A. (1993) Molecular cloning of a novel human hsp70 from a B cell line and its assignment to chromosome 5. *J. Immunol.* **151**(2), 810–813.
32. Dyer, K. D., Lavigne, M. C., and Rosenberg, H. F. (1994) Hsp70RY: Further characterization of a novel member of the hsp70 protein family. *Biochem. Biophys. Res. Commun.* **203**(1), 577–581.

33. Mizzen, L. A., Chang, C., Garrels, J. I., and Welch, W. J. (1989) Identification, characterization, and purification of two mammalian stress proteins present in mitochondria, grp 75, a member of the hsp 70 family and hsp 58, a homolog of the bacterial groEL protein. *J. Biol. Chem.* **264**(34), 20664–20675.
34. Briones, P., Vilaseca, M. A., Ribes, A., Vernet, A., Lluch, M., Cusi, V., Huckriede, A., and Agsteribbe, E. (1997) A new case of multiple mitochondrial enzyme deficiencies with decreased amount of heat shock protein 60. *J. Inherit. Metab. Dis.* **20**(4), 569–577.
35. Bonilla, E., Tanji, K., Hirano, M., Vu, T. H., DiMauro, S., and Schon, E. A. (1999) Mitochondrial involvement in Alzheimer's disease. *Biochim. Biophys. Acta* **1410**(2), 171–182.
36. Martin, J. E., Swash, M., Mather, K., and Leigh, P. N. (1993) Expression of the human groEL stress-protein homologue in the brain and spinal cord. *J. Neurol. Sci.* **118**(2), 202–206.
37. Hoyer, S. (1990) Brain glucose and energy metabolism during normal aging. *Aging (Milan)* **2**(3), 245–258.
38. Yasuno, F., Imamura, T., Hirono, N., Ishii, K., Sasaki, M., Ikejiri, Y., Hashimoto, M., Shimomura, T., Yamashita, H., and Mori, E. (1998) Age at onset and regional cerebral glucose metabolism in Alzheimer's disease. *Dement. Geriatr. Cogn. Disord.* **9**(2), 63–67.
39. Hoyer, S. (1993) Brain oxidative energy and related metabolism, neuronal stress, and Alzheimer's disease: a speculative synthesis. *J. Geriatr. Psychiatry Neurol.* **6**(1), 3–13.
40. Hamos, J. E., Oblas, B., Pulaski-Salo, D., Welch, W. J., Bole, D. G., and Drachman, D. A. (1991) Expression of heat shock proteins in Alzheimer's disease. *Neurology* **41**(3), 345–350.
41. Wartmann, M., and Davis, R. J. (1994) The native structure of the activated Raf protein kinase is a membrane-bound multisubunit complex. *J. Biol. Chem.* **269**(9), 6695–6701.
42. Brugge, J. S. (1986) Interaction of the Rous sarcoma virus protein pp60src with the cellular proteins pp50 and pp90. *Curr. Top. Microbiol. Immunol.* **123,** 1–22.
43. Pratt, W. B. (1993) The role of heat shock proteins in regulating the function, folding, and trafficking of the glucocorticoid receptor. *J. Biol. Chem.* **268**(29), 21455–21458.
44. Bohen, S. P., Kralli, A., and Yamamoto, K. R. (1995) Hold 'em and fold 'em: Chaperones and signal transduction. *Science* **268**(5215), 1303–1304.
45. Pearl, L. H., and Prodromou, C. (2000) Structure and in vivo function of Hsp90. *Curr. Opin. Struct. Biol.* **10**(1), 46–51.
46. Brown, C. R., Doxsey, S. J., Hong-Brown, L. Q., Martin, R. L., and Welch, W. J. (1996) Molecular chaperones and the centrosome. A role for TCP-1 in microtubule nucleation. *J. Biol. Chem.* **271**(2), 824–832.
47. Nagy, Z. (1999) Mechanisms of neuronal death in Down's syndrome. *J. Neural. Transm. Suppl.* **57,** 233–245.
48. Dittmar, G., Schmidt, G., Kopun, M., and Werner, D. (1997) Mapping of G2/M-phase prevalences of chaperon-encoding transcripts by means of a sensitive differential hybridization approach. *Cell. Biol. Int.* **21**(6), 383–391.
49. Roperch, J. P., Lethrone, F., Prieur, S., Piouffre, L., Israeli, D., Tuynder, M., Nemani, M., Pasturaud, P., Gendron, M. C., Dausset, J., Oren, M., Amson, R. B., and Telerman, A. (1999) SIAH-1 promotes apoptosis and tumor suppression through a network involving the regulation of protein folding, unfolding, and trafficking: identification of common effectors with p53 and p21(Waf1). *Proc. Natl. Acad. Sci. USA* **96**(14):8070–8073.